



Sequential auto-reclosing strategy for hybrid HVDC breakers in VSC-based DC grids

Xiangyu PEI¹, Guangfu TANG², Shengmei ZHANG³



Abstract The use of overhead lines for power transmission in the future high-voltage and large-capacity voltage-source converter (VSC)-based direct current (DC) grid will significantly increase the probability of temporary faults. To eliminate potential adverse impacts such as erroneous protection, line-insulation failure, and even damage to power electronic devices resulting from a DC breaker reclosing operation with the traditional sequential auto-reclosing strategy, a novel sequential auto-reclosing strategy for hybrid HVDC breakers (HHBs) in VSC-based DC grids is proposed. This strategy is based on the step-by-step operation of the transfer branch in the HHB. As a result, du/dt resulting from the HHB reclosing operation is greatly reduced, and therefore those potential negative impacts can be eliminated. Several other advantages are also presented. The feasibility and validity of the proposed strategy are verified in a four-terminal annular VSC-based DC grid electromagnetic transient model.

CrossCheck date: 26 September 2018

Received: 27 May 2018 / Accepted: 26 September 2018 / Published online: 17 December 2018
© The Author(s) 2018

✉ Xiangyu PEI
peixiangyu@geiri.sgcc.com.cn

Guangfu TANG
gftang@geiri.sgcc.com.cn

Shengmei ZHANG
zhangshengmei0104@163.com

¹ China Electric Power Research Institute, Beijing 100192, China

² Global Energy Interconnection Research Institute Co. Ltd., Beijing 102209, China

³ North China Electric Power University, Beijing 102206, China

Keywords Overhead line, Voltage-sourced converter (VSC)-based direct current grid, Temporary fault, Hybrid HVDC breaker (HHB), Auto-reclosing strategy

1 Introduction

The voltage-source converter (VSC)-based direct current (DC) grid [1–3] has been anecdotally recognized as a feasible solution for optimal allocation, wide-area reciprocity, and flexible consumption of large-scale renewable energy [4, 5]. Overhead lines (OHLs) are still considered to be the dominant transmission form for the future VSC-based DC grid. However, compared with an alternating current (AC) system, serious damage to power electronic components or the complete shutdown of a VSC-based DC grid will be caused by a steeply increasing fault current, owing to the low impedance of a short-circuit path [6–8]. Moreover, temporary faults will be more likely because of the use of OHLs in unpredictable and harsh environments. Consequently, both fault isolation and system recovery are crucial problems [9–11] urgently to be solved in the construction of the high-voltage and large-capacity VSC-based DC grid.

A variety of fault-isolation and system-recovery schemes have been proposed. They can be broadly divided into two technical routes. One is based on converters incapable of fault current interruption and DC breakers (DCBs) [12–15]. Fault isolation and system recovery are mainly realized by the fast operation of the corresponding DCBs. The other is based on converters capable of fault current interruption [16–21] and an ultrafast mechanical switch (UMS). The fault current is first interrupted by converters. Then the fault section is isolated by the UMS. System recovery is achieved by their coordinated

operation. The former route appears to be more competitive for the VSC-based DC grid in regards to the continuous and reliable transmission of active power.

Research of the former route primarily focuses on fault analysis [22, 23], protection schemes [24–30], fault location [31–34], and protection coordination [35], generally to the exclusion of system-recovery strategies. Similar to an AC system, system recovery of the VSC-based DC grid can be realized by the reclosing operation of DCBs. However, based on different working principles, the breaking time of an AC breaker is typically 40–60 ms, while that of a DCB can be as fast as 3 ms. Moreover, unlike an AC system, the DC system has no natural zero-crossing point. Therefore, reclosing in the DC system should be reconsidered.

Synchronous operation of the transfer branch in a hybrid HVDC breaker (HHB) [36] has been proposed to reduce the adverse effects on the VSC-based DC grid from a DCB reclosing operation under a permanent fault [37]. Specifically, all fully-controlled fast-power electronic switches in the transfer branch are energized to carry out the reclosing operation synchronously. Then the main branch is conducted if no fault is detected. Conversely, once a permanent fault is detected, all the fully-controlled fast-power electronic switches in the transfer branch will be immediately de-energized synchronously to interrupt the fault current. We call this the traditional sequential auto-reclosing strategy in this paper, and with its help, the fault current can be interrupted immediately if a permanent fault is detected. However, potential negative impacts such as erroneous protection, line-insulation failure, and even damage to power electronic devices will occur when the fault is temporary.

To eliminate these potential negative impacts in the system-recovery procedure, a novel sequential auto-reclosing strategy for HHBs in VSC-based DC grids is proposed in this paper. Based on the step-by-step operation of the transfer branch, this strategy eliminates potential negative impacts of the traditional sequential auto-reclosing strategy, and has several other advantages.

The remainder of this paper is organized as follows. Section 2 describes the overall protection-operation sequence for the DC line and the sequential operation sequence of the HHB, and analyzes the energy dissipated by the metal oxide varistor (MOV) in each unit. In Section 3, based on the traditional sequential auto-reclosing strategy, the novel sequential auto-reclosing strategy is proposed. Theoretical analysis of the two strategies is discussed in Section 4. The PSCAD/EMTDC simulation verification is performed in Section 5. Section 6 makes concluding remarks.

2 Basic principle

2.1 Overall protection operation sequence

The overall protection operation sequence based on the former technical route is shown in Fig. 1. The DC line-protection system identifies a fault within 3 ms and sends a protection action order to the local DCB, which completes its breaking operation within 3 ms after receiving the order. The fault line finishes the deionization to recover its insulation within about 300 ms. The local DCB executes its reclosing operation after the insulation recovery. If the fault has been cleared, the VSC-based DC grid will resume its normal power. Otherwise, the local DCB will break again to isolate the fault line.

The overall protection operation sequence is as follows.

- 1) t_0 : DC line fault inception.
- 2) t_{0-t_1} : fault identification by line-protection system.
- 3) t_1 : protection action order is sent to the local DCB.
- 4) t_{1-t_2} : DCB breaking operation.
- 5) t_{2-t_3} : fault-line deionization to recover its insulation.
- 6) t_3 : DCB starts its reclosing operation.
- 7) t_{3-t_4} : DCB executes its reclosing operation. If the operation is successful, then the system will resume its normal power after a certain time and procedure t_4-t_5 will be skipped.
- 8) t_{4-t_5} : if the DCB reclosing operation is unsuccessful, the DCB will break again to isolate the fault line.

2.2 Sequential operation sequence of HHB

As shown in Fig. 2, the HHB based on the cascaded diode full-bridge module consists of main, transfer, and absorption branches [38]. The main branch, which is composed of an UMS with multi-breaks and a small number of power electronic modules (PEMs), mainly conducts load current in normal operation and assists in transferring fault current in the DCB breaking operation. The transfer branch consists of hundreds of PEMs in series, and is mainly utilized to bear the fault current in a short time and establish the transient breaking voltage. The absorption branch is composed of MOVs and is used to suppress the transient breaking voltage and dissipate the energy stored in the system.

The sequential operation sequence of the HHB is shown in Fig. 3, where i_{main} , i_{transfer} and i_{MOV} denote the current

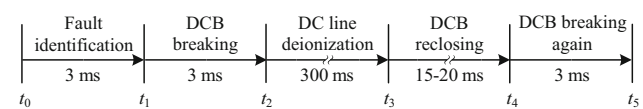


Fig. 1 Overall protection operation sequence

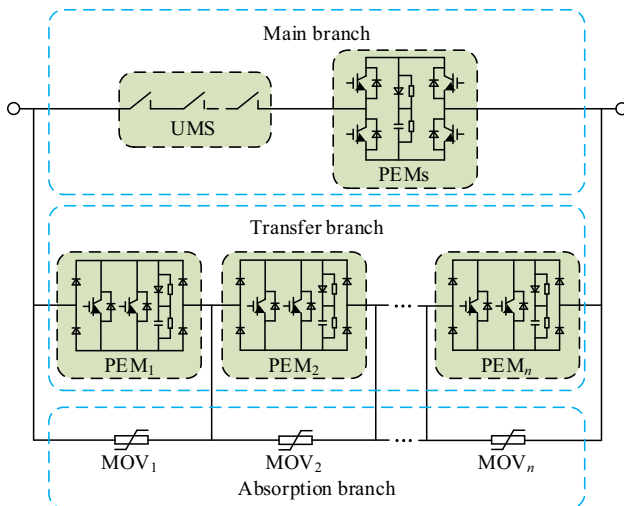


Fig. 2 Basic structure of HHB

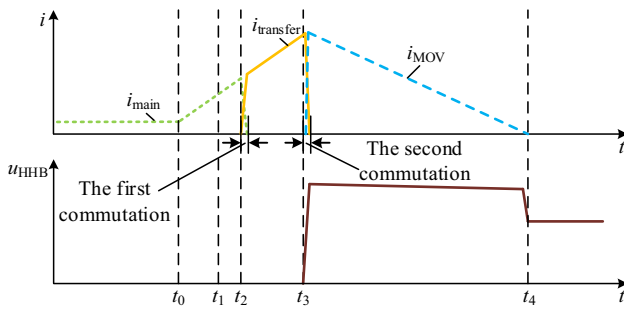


Fig. 3 Sequential operation sequence of HHB

of the main branch, transfer branch and absorption branch respectively, and u_{HHB} denotes the port-voltage of HHB.

- 1) t_0 : DC line-fault inception.
- 2) t_1 : local HHB receives the protection action order from the DC line-protection system.
- 3) t_2 : local HHB starts the first commutation to force the fault current to shift from its main branch to its transfer branch.
- 4) t_3 : local HHB starts the second commutation to force the fault current to shift from its transfer branch to its absorption branch. The port-voltage of HHB rises from zero to a higher protective voltage U_{MOV} in a very short time due to the triggered MOVs in the absorption branch.
- 5) t_4 : the fault current is forced to zero with the help of the higher protective voltage U_{MOV} , and the port-voltage of HHB equals the DC bus voltage U_{dc} after its breaking operation.

2.3 Energy dissipated by MOV in each unit

When a short-circuit fault f near S_1 occurs on Line₁₂ in the three-terminal MMC-HVDC system shown in Fig. 4, the fault current flowing through HHB₁₂ will rise sharply.

Referring to the sequential operation sequence of the HHB shown in Fig. 3, the fault current mainly contributed by MMC in S_1 can be expressed as:

$$i_{f12}(t) = I_{12} + \frac{V_1}{L_{\text{loop}}}(t - t_0) \quad (1)$$

where I_{12} is the pre-faulted steady-state current of Line₁₂; V_1 is the DC voltage of the MMC in S_1 ; and L_{loop} is the total fault loop inductance.

For HHB₁₂, the peak currents of the main branch and transfer branch appear at t_2 and t_3 respectively, and can be calculated as:

$$i_{fMB} = I_{12} + \frac{V_1}{L_{\text{loop}}}(t_2 - t_0) \quad (2)$$

$$i_{fTB} = I_{12} + \frac{V_1}{L_{\text{loop}}}(t_3 - t_0) \quad (3)$$

As shown in Fig. 3, the voltage can be assumed to be constant at the protection level during t_3-t_4 for the MOV in each unit. The maximum energy dissipated by the MOV in each unit can be calculated as:

$$E_{\text{MOV}} = \frac{t_4 - t_3}{2} V_{\text{MOV}} i_{fTB} \quad (4)$$

where V_{MOV} is the rated protective voltage of the MOV in each cascaded unit.

3 Sequential auto-reclosing strategies

The auto-reclosing transient procedure of the HHB is shown in Fig. 5. The initial states of HHB_M and HHB_N are both open. To illustrate, HHB_M near DC bus M is taken as an example. The state of HHB_M reclosing in Fig. 5a can be revealed by the equivalent circuit in Fig. 5b, where two DC

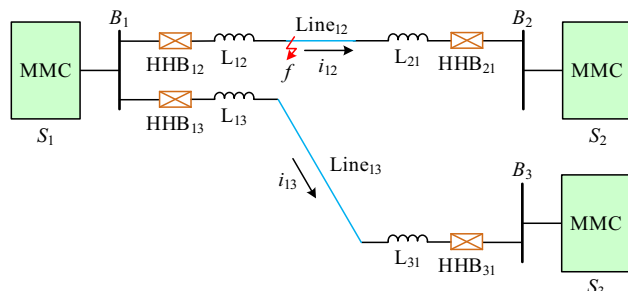


Fig. 4 One-line diagram of a three-terminal MMC-HVDC system



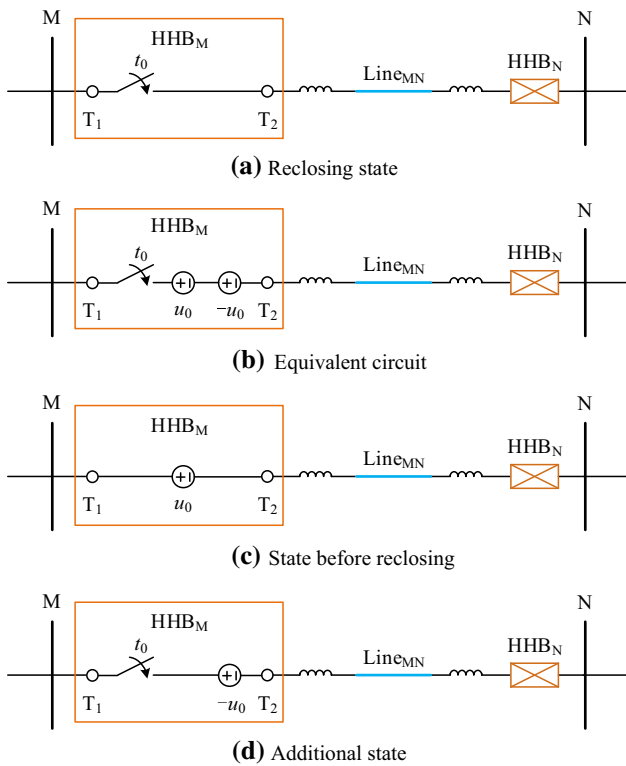


Fig. 5 HHB reclosing operation

voltage sources with equal amplitude but opposite polarity are connected in series. According to the superposition principle, the equivalent circuit shown in Fig. 5b can be decomposed into two states: the state before reclosing and an additional state, as shown in Fig. 5c, d, respectively. In the state before reclosing shown in Fig. 5c, u_0 equals the voltage difference between DC bus M and DC line Line_{MN}. As shown in Fig. 5d, a DC voltage source $-u_0$ will be connected to the DC system in series at t_0 .

3.1 Traditional auto-reclosing strategy

The traditional auto-reclosing strategy [33] for the HHB is shown in Fig. 6. In this strategy, PEMs in the main branch are energized after the fault current is interrupted by MOVs in the absorption branch. Having waited for the predetermined deionization period for insulation recovery, the HHB performs its reclosing operation.

As shown in Fig. 6, the initial states of the PEMs and UMS in the main branch are closed and open, respectively. Those of PEM_i ($i = 1, 2, \dots, n$) in the transfer branch are all open. The traditional sequential auto-reclosing sequence is as follows.

- 1) t_0 : all PEM_i in the transfer branch are energized at the same time. If the fault has been cleared, then there will no fault current to be detected. Once a fault current is

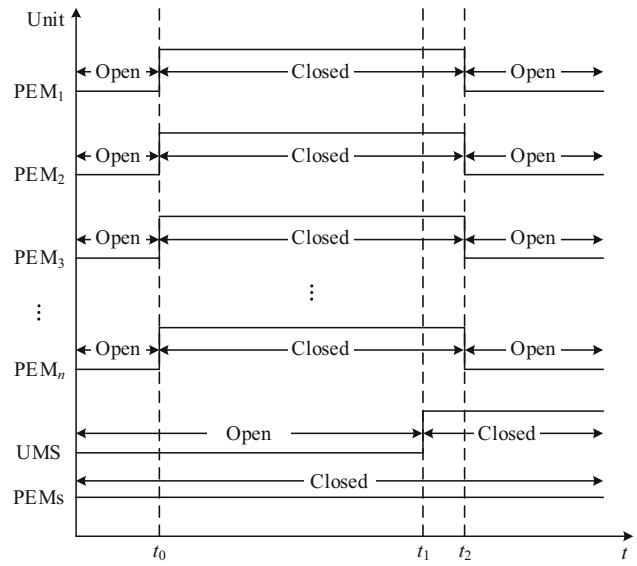


Fig. 6 Traditional auto-reclosing strategy

detected, all PEM_i ($i = 1, 2, \dots, n$) in the transfer branch are de-energized synchronously again, and the next procedure will be skipped.

- 2) t_1 : if all PEM_i in the transfer branch are energized successfully, then the UMS in the main branch will be energized.
- 3) t_2 : all PEM_i in the transfer branch are de-energized at the same time. As a result, the main branch of the HHB is in a conducting state.

It can be concluded from the additional state shown in Fig. 5d that the larger DC voltage source $-u_0$ suddenly connected to the DC system in series at t_0 will result in a larger du/dt under a temporary fault, which will negatively influence the whole VSC-based DC grid. Specifically, the larger du/dt may cause erroneous protection. Moreover, the resultant voltage oscillation may cause line-insulation failure and even damage to power electronic devices. To eliminate these potential adverse impacts, it is necessary to redesign the sequential auto-reclosing strategy and propose an optimal sequential auto-reclosing strategy.

3.2 Proposed auto-reclosing strategy

The proposed sequential auto-reclosing strategy is based on the step-by-step operation of the PEMs in the transfer branch of the HHB. As shown in Fig. 7, the initial states of the PEMs, UMS, and PEM_i ($i = 1, 2, \dots, n$) are the same as those in the traditional auto-reclosing strategy. The proposed sequential auto-reclosing sequence is as follows.

- 1) t_0 : PEM₁ in the transfer branch is energized to bypass MOV₁. If the fault has been cleared, then there will be no fault current to be detected. If the fault is

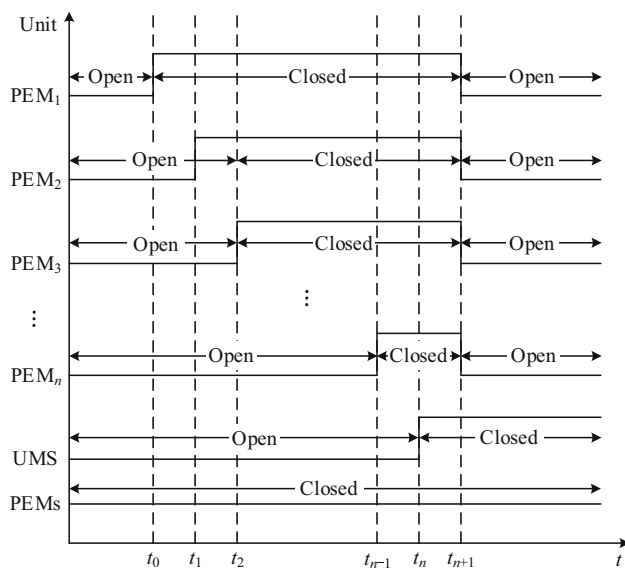


Fig. 7 Proposed auto-reclosing strategy

permanent, then the remaining MOVs that have not been bypassed may be triggered, and a fault current will occur. Once the fault current is detected, PEM_1 in the transfer branch will be de-energized immediately, and the following procedures will be skipped.

- 2) t_1 : PEM_2 in the transfer branch is energized to bypass MOV_2 . Once a fault current is detected, PEM_1 and PEM_2 in the transfer branch will be de-energized immediately, and the next procedures will be skipped.
- 3) t_2 : PEM_3 in the transfer branch is energized to bypass MOV_3 . Once a fault current is detected, PEM_1 , PEM_2 , and PEM_3 in the transfer branch will be de-energized immediately, and the next procedures will be skipped.
- 4) t_{n-1} : PEM_n in the transfer branch is energized to bypass MOV_n . Once a fault current is detected, all PEM_i ($i = 1, 2, \dots, n$) in the transfer branch will be de-energized immediately, and the next procedures will be skipped.
- 5) t_n : if all PEM_i ($i = 1, 2, \dots, n$) in the transfer branch are energized successfully and no fault current has been detected, then the UMS in the main branch will be energized.
- 6) t_{n+1} : all PEM_i ($i = 1, 2, \dots, n$) in the transfer branch are de-energized at the same time. As a result, the main branch of the HHB is in a conducting state.

Using the proposed strategy, it is obvious that the DC voltage source $-u_0$ is gradually connected to the DC system in series at time intervals between t_0 and t_{n-1} under a temporary fault. Compared with the traditional auto-reclosing strategy, the resultant du/dt can be considerably reduced. Therefore, potential negative impacts caused by

the HHB reclosing with the traditional auto-reclosing strategy can be eliminated.

4 Theoretical analysis

The HHB auto-reclosing operation is shown in Fig. 8. The initial voltage of terminal T_1 connected with the MMC is equivalent to a DC voltage source V_1 , while that of terminal T_2 connected with the transmission line is nearly zero. In essence, DC lines connected with terminals T_1 and T_2 of the HHB are connected through the absorption branch operating in a small-current zone.

The reclosing operation based on the traditional strategy is shown in Fig. 9. Essentially, T_1 and T_2 are suddenly short-circuited by a wire at t_0 . It can be concluded from the addition state shown in Fig. 5d that whether the fault is temporary or permanent, there must be a DC voltage source $-V_1$ suddenly connected to the DC line in series at the same time. The resultant larger du/dt will negatively influence the whole system, especially under a temporary fault.

The reclosing operation based on the proposed strategy is shown in Fig. 10. The cascaded MOVs are gradually bypassed by the corresponding PEMs in the transfer branch from time t_0 to t_n step by step. If the fault is temporary, then the transmission line will be charged through MOVs that are not yet bypassed, and as a result, the voltage V_{Line} will gradually increase from zero to V_1 , and du/dt can be mostly reduced. If the fault is permanent, then V_{Line} will always be zero. When MOV_k is bypassed at time t_{k-1} , the remaining MOVs will be triggered because of their lower protection level in the reclosing procedure.

The equivalent circuit under a permanent fault is shown in Fig. 11. The equivalent DC voltage and resistance of the triggered MOVs are V_0 and R_0 , respectively. The protection level V_0 of the triggered MOVs is:

$$V_0 = (n - k)V_{\text{MOV}} \quad (5)$$

It can be concluded from the addition state shown in Fig. 5d and the equivalent circuit shown in Fig. 11 that the equivalent DC voltage source $-(V_1 - V_0)$ suddenly

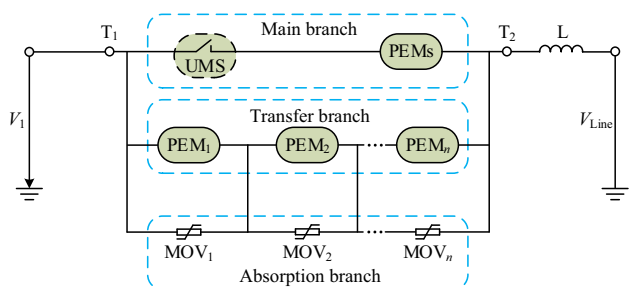


Fig. 8 Initial state of HHB auto-reclosing operation



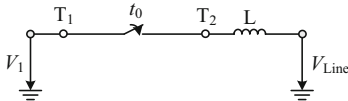


Fig. 9 Operation based on traditional auto-reclosing strategy

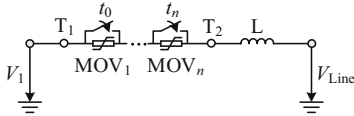


Fig. 10 Operation based on proposed auto-reclosing strategy

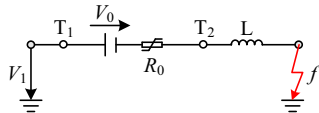


Fig. 11 Equivalent circuit for the proposed strategy under permanent fault

connected to the DC system in series at time t_{k-1} , will be greatly reduced.

In summary, whether the fault is temporary or permanent, the resultant du/dt can be mostly reduced by the proposed auto-reclosing strategy, eliminating the potential negative impacts resulting from the HHB reclosing with the traditional auto-reclosing strategy.

5 Simulation verification

To verify the feasibility and validity of the proposed sequential auto-reclosing strategy, a ± 500 kV four-terminal annular VSC-based DC grid electromagnetic transient model, as shown in Fig. 12, is built in the PSCAD/EMTDC environment. The VSC-based DC grid operates in rigid bipolar mode with a metallic return, which is grounded through a resistance of 15Ω in converter station S_4 . The frequency-dependent line model is adopted for all 500 kV OHLs. The main parameters of the VSC-based DC grid and control modes of the four converter stations are shown in Tables 1 and 2, respectively. The transfer branch and absorption branch of each HHB are divided into 10 cascaded units with the same characteristics on average. The time interval between each two successive enabling pulses for PEMs in the transfer branch is 2 ms.

The performance of the proposed strategy is evaluated in the VSC-based DC grid electromagnetic transient model under typical faults including pole-to-ground and pole-to-pole short-circuit faults. These two typical faults are set in the middle position of OHL₃₄ at $t = 2$ s. About 3 ms later, HHB₃₄ and HHB₄₃ receive protection-action orders from their local line-protection systems and perform their

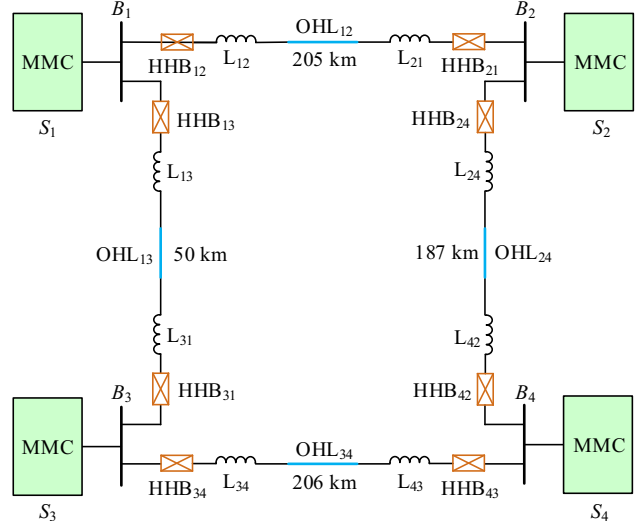


Fig. 12 ± 500 kV four-terminal annular VSC-based DC grid

breaking operations. At about $t = 2.006$ s, the fault current begins to decrease from the peak value to zero in 10–20 ms. It should be noted that there is no MMC blocking in this procedure. After the predetermined deionization period of 300 ms, HHB₃₄ starts its sequential auto-reclosing operation. If this is successful, then HHB₄₃ implements its sequential auto-reclosing operation, referring to the sequential auto-reclosing strategies of the AC circuit breaker. The simulation results based on these two kinds of sequential auto-reclosing strategies under the typical faults are analyzed.

5.1 Performance under pole-to-ground short-circuit fault

5.1.1 Temporary fault

The control signals for PEMs in transfer branch under a temporary pole-to-ground fault and the simulation results based on the two kinds of sequential auto-reclosing strategies are shown in Figs. 13 and 14 for the case of setting the duration time of a temporary positive pole-to-ground short-circuit fault of less than 300 ms.

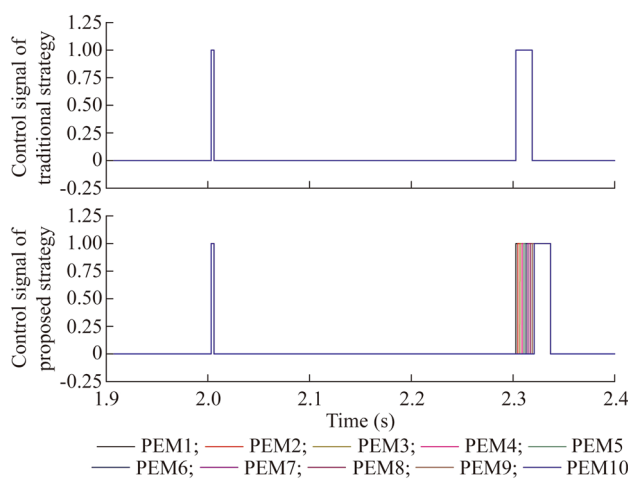
As shown in Fig. 13, the control signals for PEMs in the transfer branch with the traditional strategy operate synchronously, while those with the proposed strategy operate step by step. In Fig. 14a, the port voltage of HHB₃₄, locating at the positive-pole line with the traditional strategy, decreases to zero vertically, while with the proposed strategy, it gradually reduces to 0 with a ramp. In Fig. 14b, an obvious current oscillation occurs in the same HHB₃₄ branch currents with the traditional strategy, while there is almost no current oscillation with the proposed strategy. As shown in Fig. 14c, a large voltage oscillation, with a

Table 1 Main parameters of VSC-based DC grid

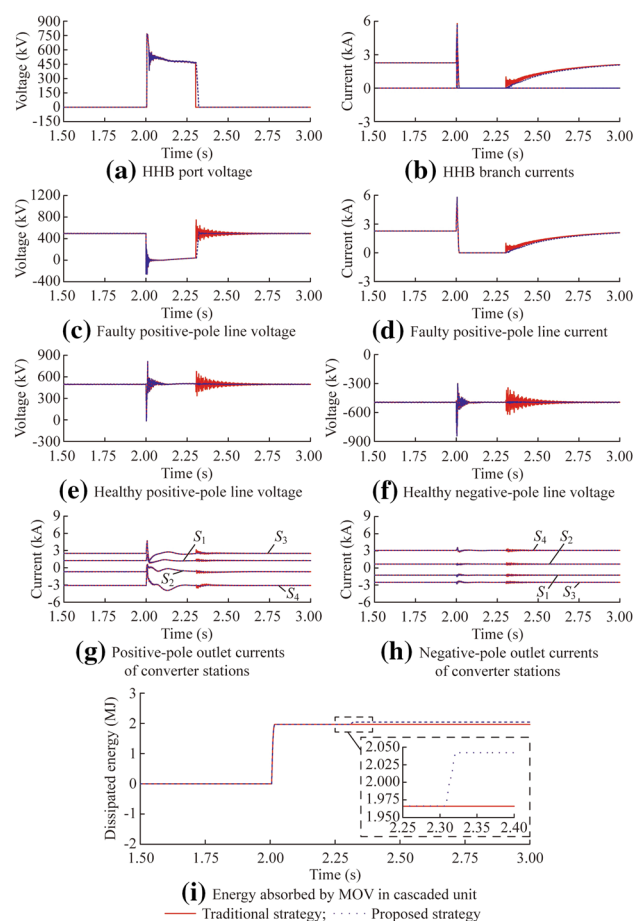
| Converter station | Operation mode | Rated capacity (MVA) | Rated DC voltage (kV) | Rated AC voltage (kV) | SCR | Transformer ratio | Arm inductance (mH) | SM number | Redundancy (%) | SM capacitance (mF) |
|-------------------|----------------|----------------------|-----------------------|-----------------------|-----|-------------------|---------------------|-----------|----------------|---------------------|
| S_1 | Bipolar | 1700 | ± 500 | 220 | 5 | 220/275 | 100 | 264 | 8 | 8 |
| S_2 | Bipolar | 1700 | ± 500 | 500 | 5 | 500/275 | 100 | 264 | 8 | 8 |
| S_3 | Bipolar | 3400 | ± 500 | 220 | 5 | 220/275 | 50 | 264 | 8 | 15 |
| S_4 | Bipolar | 3400 | ± 500 | 500 | 5 | 500/275 | 50 | 264 | 8 | 15 |

Table 2 Control modes of four converter stations

| Converter station | P (MW) | U_{dc} (kV) | Q (Mvar) | U_{ac} (kV) |
|-------------------|----------|---------------|------------|---------------|
| S_1 | 1250 | | 0 | |
| S_2 | | ± 500 | 0 | |
| S_3 | 2500 | | 0 | |
| S_4 | -3000 | | 0 | |

**Fig. 13** Control signals for PEMs in transfer branch under a temporary pole-to-ground fault

maximum value up to about 1.55 p.u. of the rated DC voltage, occurs in the fault line with the traditional strategy, yet there is almost no voltage oscillation with the proposed strategy. In Fig. 14d, the current waveforms of the fault line with the corresponding auto-reclosing strategy are the same as in Fig. 14e because the HHBs are connected with the DC lines in series. As shown in Fig. 14e, f, larger voltage oscillations are discovered in the healthy pole lines with the traditional strategy, but there are no obvious voltage oscillations with the proposed strategy. In Fig. 14g, h, obvious oscillations are observed in the outlet currents of all the converter stations with the traditional strategy, while there are almost no current oscillations in the outlet currents of the four converter stations

**Fig. 14** Simulation results under a temporary pole-to-ground fault

with the proposed strategy. As shown in Fig. 14i, no energy is absorbed by the MOV in the cascaded unit with the traditional strategy, while energy absorbed by the MOV in the cascaded unit with the proposed strategy is discovered in the same HHB_{34} auto-reclosing procedure. However, the dissipated energy with the proposed strategy is still within the tolerance of the corresponding MOV, and could be ignored when compared to that in the same HHB_{34} breaking procedure.



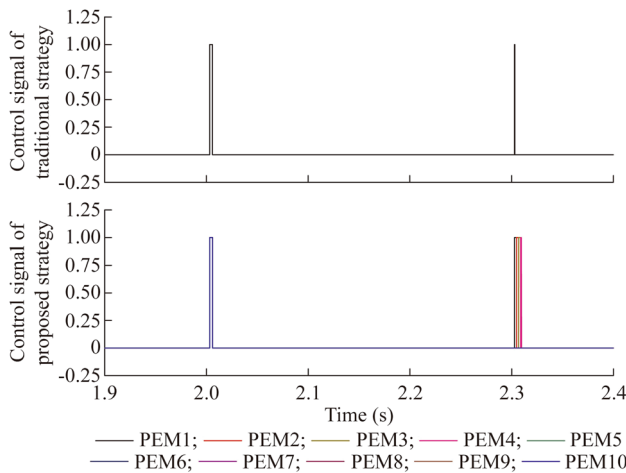


Fig. 15 Control signals for PEMs in transfer branch under a temporary pole-to-ground fault

5.1.2 Permanent fault

The control signals for PEMs in transfer branch under a temporary pole-to-ground fault and the simulation results based on the two kinds of sequential auto-reclosing strategies are shown in Figs. 15 and 16 for the case when the positive pole-to-ground short-circuit fault is permanent.

As shown in Fig. 15, a permanent fault is detected immediately with the traditional strategy, while with the proposed strategy, it is not detected until the MOVs that have not been bypassed are triggered. Once the fault is detected, the control signals for PEMs in the transfer branch are de-energized immediately. In Fig. 16a, a larger oscillation in the port-voltage of HHB₃₄ at the positive-pole line is observed after the voltage decreases to zero vertically with the traditional strategy, while with the proposed strategy, a smaller voltage oscillation is discovered due to the voltage caused by the triggered MOVs that have not been bypassed. In Fig. 16b, the fault current flowing through the same HHB₃₄ is detected somewhat earlier with the traditional strategy. The current occurring in the reclosing procedure is much smaller than the peak current in the breaking procedure. As shown in Fig. 16c, the voltage oscillation amplitude of the fault line with the traditional strategy is larger than that with the proposed strategy. In Fig. 16d, the current waveforms of the fault line with the corresponding auto-reclosing strategy are the same as those in Fig. 16b, again because the HHBs are connected with DC lines in series. As shown in Fig. 16e, f, the voltages of healthy pole lines show a larger oscillation with the traditional strategy than those with the proposed strategy. In Fig. 16g, h, no obvious oscillation is observed in the outlet currents of all the converter stations with either strategy. As shown in Fig. 16i, the maximum energy

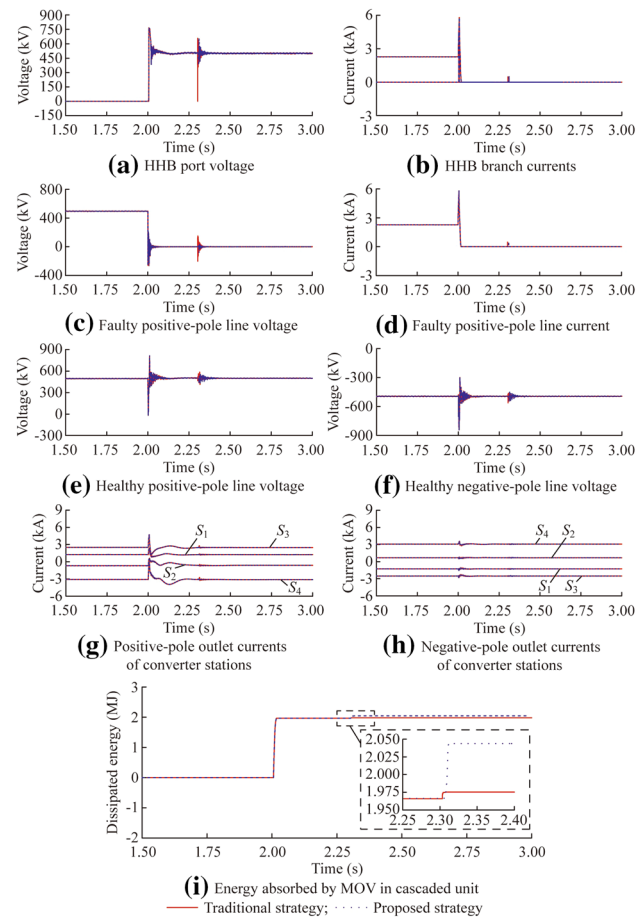


Fig. 16 Simulation results under a permanent pole-to-ground fault

absorbed by MOV in a cascaded unit is larger with the proposed strategy than that with the traditional strategy in the same HHB₃₄ auto-reclosing procedure. However, the dissipated energy is still within the tolerance of the corresponding MOV and can be ignored when compared to that in the same HHB₃₄ breaking procedure.

5.2 Performance under pole-to-pole short-circuit fault

5.2.1 Temporary fault

Simulation results based on the two kinds of sequential auto-reclosing strategies are shown in Fig. 17 for the case of setting the duration time of a temporary pole-to-pole short-circuit fault of less than 300 ms.

The control signals omitted here for PEMs in the transfer branch with both strategies are the same as those shown in Fig. 13. In Fig. 17a, the port voltage of HHB₃₄ in the positive-pole line with the traditional strategy decreases to zero vertically, while that with the proposed strategy gradually reduces to zero with a ramp, which is the same as

in Fig. 14a. As shown in Fig. 17b–f, branch currents of the same HHB₃₄, faulty positive-pole line voltage, faulty positive-pole line current, healthy positive-pole voltage, and positive-pole outlet currents of the four converter stations with the traditional strategy show larger oscillations than those with the proposed strategy. It is worth noting that large voltage oscillations with peak values up to about 1.68 p.u. and 1.65 p.u. of the rated DC voltage respectively occur in the faulty positive-pole line shown in Fig. 17c and healthy positive-pole line between S_1 and S_2 shown in Fig. 17e with the traditional strategy, while no obvious voltage oscillation is observed in the same lines with the proposed strategy. In Fig. 17g, no energy is absorbed by the MOV in a cascaded unit with the traditional strategy, while the energy absorbed with the proposed strategy is within tolerance of the MOV and can be ignored when compared to that in the same HHB₃₄ breaking procedure.

5.2.2 Permanent fault

The simulation results based on the two kinds of sequential auto-reclosing strategies are shown in Fig. 18 for the case when the pole-to-pole short-circuit fault is permanent.

The control signals omitted here for PEMs in the transfer branch with both strategies are the same as those shown in Fig. 15. In Fig. 18a, a larger oscillation in the port voltage of HHB₃₄ in the positive-pole line is observed after the voltage decreases to zero vertically with the traditional strategy, while with the proposed strategy, a smaller voltage oscillation is discovered due to the voltage from triggered MOVs that have not been bypassed, which is the same as in Fig. 16a. As shown in Fig. 18b, d, the fault current, which is much smaller than the peak current in the breaking procedure flowing through the same HHB₃₄ and faulty positive-pole line, is detected somewhat earlier with the traditional strategy. In Fig. 18c, e, a faulty positive-pole line voltage and healthy positive-pole voltage show larger oscillations with the traditional strategy than those with the proposed strategy, and are the same as those under a permanent pole-to-ground fault. As shown in Fig. 18f, no obvious oscillation is observed in the positive-pole outlet currents of all the converter stations with either strategy. In Fig. 18g, the maximum energy absorbed by the MOV in a cascaded unit is larger with the proposed strategy than that with the traditional strategy. However, the dissipated energy is still within tolerance of the corresponding MOV, and can be ignored when compared with that in the same HHB₃₄ breaking procedure.

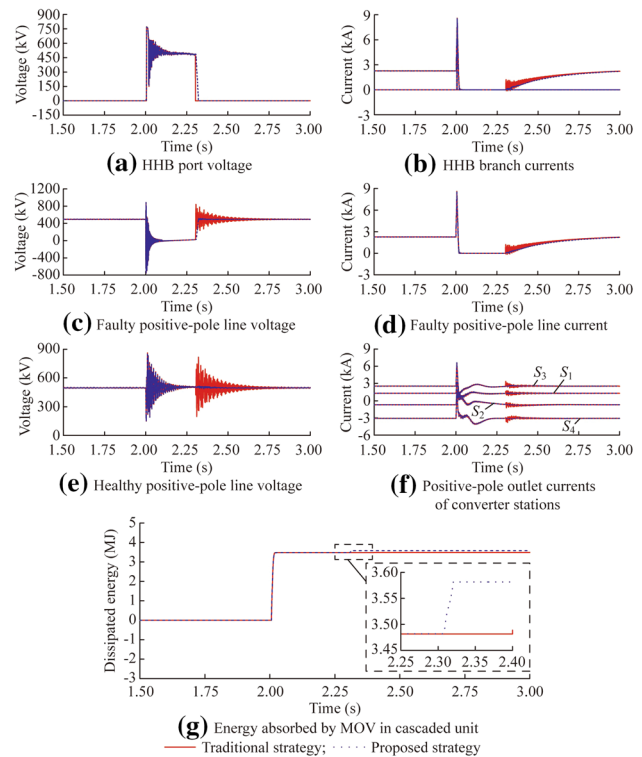


Fig. 17 Simulation results under a temporary pole-to-pole fault

5.3 Applicability analysis

Based on the simulations of both sequential auto-reclosing strategies with typical faults, the proposed strategy performs better overall than the traditional strategy, especially under temporary faults with a higher probability, because of the use of OHLs.

To avoid more negative impacts on the whole VSC-based DC grid, the HHB auto-reclosing operation based on the traditional strategy should be performed from one side of the DC line. If the auto-reclosing operation is successful and the normal voltage is restored, then the HHB on the other side of the DC line can be reclosed. In addition, if the communication for the HHB auto-reclosing operation between two sides of the DC line is a failure, then there will be a false order for the corresponding HHB and an even greater influence on the whole VSC-based DC grid.

However, the HHB auto-reclosing operation based on the proposed strategy not only can be performed from one side, but can simultaneously be carried out from two sides of the DC line, and the communication for the HHB auto-reclosing operation between two sides of the DC line can be omitted economically. In addition, multiple auto-reclosing operations can be executed because the negligible dissipated energy is still within the tolerance of the corresponding MOV. Moreover, the time consumed for the



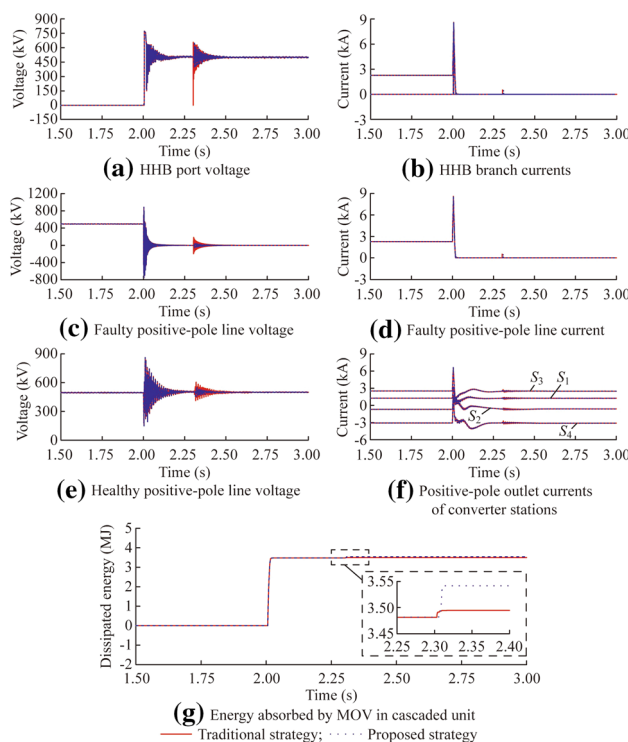


Fig. 18 Simulation results under a permanent pole-to-pole fault

HHB auto-reclosing can be neglected compared with the predetermined deionization period for insulation recovery.

6 Conclusion

A novel sequential auto-reclosing strategy for HHBs in VSC-based DC grids is proposed. This strategy is based on the step-by-step operation of the PEMs in the transfer branch of the HHB. The overall performance of the HHB with the proposed strategy is better than that with the traditional strategy, especially under a temporary fault with a higher probability because of the use of OHLs.

The resultant dU/dt is largely reduced with the proposed sequential auto-reclosing strategy, and therefore those potential adverse impacts can be eliminated. The HHB auto-reclosing operation based on the proposed sequential auto-reclosing strategy not only can be performed from one side of the DC line, but can be carried out from two sides simultaneously. Also, communication for the HHB auto-reclosing operation between two sides of the DC line can be omitted economically. Multiple auto-reclosing operations can be executed because of the negligible dissipated energy, and time consumption can be neglected compared with the predetermined deionization period for insulation recovery.

Acknowledgements This work was supported by National Key R&D Program of China (No. 2017YFB0902400).

Open Access This article is distributed under the terms of the Creative Commons Attribution 4.0 International License (<http://creativecommons.org/licenses/by/4.0/>), which permits unrestricted use, distribution, and reproduction in any medium, provided you give appropriate credit to the original author(s) and the source, provide a link to the Creative Commons license, and indicate if changes were made.

References

- [1] Ajaei FB, Iravani R (2016) Cable surge arrester operation due to transient overvoltages under DC-side faults in the MMC-HVDC link. *IEEE Trans Power Deliv* 31(3):1213–1222
- [2] Flourentzou N, Agelidis VG, Demetriadis GD (2009) VSC-based HVDC power transmission systems: an overview. *IEEE Trans Power Electron* 24(3):592–602
- [3] Zheng XD, Tai NL, Wu ZY et al (2014) Harmonic current protection scheme for voltage source converter-based high-voltage direct current transmission system. *IET Gen Transm Distrib* 8(9):1509–1515
- [4] Geddada N, Yeap YM, Ukil A (2018) Experimental validation of fault identification in VSC-based DC grid system. *IEEE Trans Ind Electron* 65(6):4799–4809
- [5] Wan X, Li YF, Peng MF (2018) Modelling, analysis and virtual parallel resistor damping control of VSC-based DC grid using master-slave control mode. *IET Gen Transm Distrib* 12(9):2046–2054
- [6] Wang J, Ma H, Bai ZH (2018) A submodule fault ride-through strategy for modular multilevel converters with nearest level modulation. *IEEE Trans Power Electron* 33(2):1597–1608
- [7] Li R, Xu L, Holliday D et al (2016) Continuous operation of radial multiterminal HVDC systems under DC fault. *IEEE Trans Power Deliv* 31(1):351–361
- [8] Rodriguez P, Rouzebehi K (2017) Multi-terminal DC grids: challenges and prospects. *J Mod Power Syst Clean Energy* 5(4):515–523
- [9] Xue YL, Xu Z (2014) On the bipolar MMC-HVDC topology suitable for bulk power overhead line transmission: configuration, control, and DC fault analysis. *IEEE Trans Power Deliv* 29(6):2420–2429
- [10] Hu JB, Xu KC, Lin L et al (2017) Analysis and enhanced control of hybrid-MMC-based HVDC systems during asymmetrical DC voltage faults. *IEEE Trans Power Deliv* 32(3):1394–1403
- [11] Li XQ, Song Q, Liu WH et al (2013) Protection of nonpermanent faults on DC overhead lines in MMC-based HVDC systems. *IEEE Trans Power Deliv* 28(1):483–490
- [12] Shan YH, Lim TC, Finney SJ et al (2017) Cascaded commutation circuit for a hybrid DC breaker with dynamic control on fault current and DC breaker voltage. *IET Power Electron* 10(6):676–686
- [13] Majumder R, Auddy S, Berggren B et al (2017) An alternative method to build DC switchyard with hybrid DC breaker for DC grid. *IEEE Trans Power Deliv* 32(2):713–722
- [14] Wang WY, Barnes M, Marjanovic O et al (2016) Impact of DC breaker systems on multiterminal VSC-HVDC stability. *IEEE Trans Power Deliv* 31(2):769–779
- [15] Sneath J, Rajapakse AD (2016) Fault detection and interruption in an earthed HVDC grid using ROCOV and hybrid DC breakers. *IEEE Trans Power Deliv* 31(3):973–981

- [16] Zhang JP, Zhao CY (2015) The research of SM topology with DC fault tolerance in MMC-HVDC. *IEEE Trans Power Deliv* 30(3):1561–1568
- [17] Xue YL, Xu Z, Tu QR (2012) Modulation and control for a new hybrid cascaded multilevel converter with DC blocking capability. *IEEE Trans Power Deliv* 27(4):2227–2237
- [18] Cui SH, Sul SK (2016) A comprehensive DC short-circuit fault ride through strategy of hybrid modular multilevel converters (MMCs) for overhead line transmission. *IEEE Trans Power Electron* 31(11):7780–7796
- [19] Li R, Adam GP, Holliday D et al (2015) Hybrid cascaded modular multilevel converter with DC fault ride-through capability for the HVDC transmission system. *IEEE Trans Power Deliv* 30(4):1853–1862
- [20] Merlin MMC, Green TC, Mitcheson PD et al (2014) The alternate arm converter: a new hybrid multilevel converter with DC-fault blocking capability. *IEEE Trans Power Deliv* 29(1):310–317
- [21] Qin JC, Saeedifard M, Rockhill A et al (2015) Hybrid design of modular multilevel converters for HVDC systems based on various submodule circuits. *IEEE Trans Power Deliv* 30(1):385–394
- [22] Wang M, Beerten J, Hertem DV (2017) Frequency domain based DC fault analysis for bipolar HVDC grids. *J Mod Power Syst Clean Energy* 5(4):548–559
- [23] Li B, He JW, Tian J et al (2017) DC fault analysis for modular multilevel converter-based system. *J Mod Power Syst Clean Energy* 5(2):275–282
- [24] Liu J, Tai NL, Fan CJ (2017) Transient-voltage-based protection scheme for DC line faults in the multiterminal VSC-HVDC system. *IEEE Trans Power Deliv* 32(3):1483–1494
- [25] Tzelepis D, Dysko A, Fusiek G et al (2017) Single-ended differential protection in MTDC networks using optical sensors. *IEEE Trans Power Deliv* 32(3):1605–1615
- [26] Lewis PT, Grainger BM, Hassan HAA et al (2016) Fault section identification protection algorithm for modular multilevel converter-based high voltage DC with a hybrid transmission corridor. *IEEE Trans Ind Electron* 63(9):5652–5662
- [27] Kerf KD, Srivastava K, Reza M et al (2011) Wavelet-based protection strategy for DC faults in multi-terminal VSC HVDC systems. *IET Gen Transm Distrib* 5(4):496–503
- [28] Mobarrez M, Kashani MG, Bhattacharya S (2016) A novel control approach for protection of multiterminal VSC-based HVDC transmission system against DC faults. *IEEE Trans Ind Appl* 52(5):4108–4116
- [29] Li SL, Chen W, Yin XG et al (2017) Protection scheme for VSC-HVDC transmission lines based on transverse differential current. *IET Gen Transm Distrib* 11(11):2805–2813
- [30] Pei XY, Tang GF, Zhang SM (2018) A novel pilot protection principle based on modulus traveling-wave currents for voltage-sourced converter based high voltage direct current (VSC-HVDC) transmission lines. *Energies* 11(9):2395
- [31] Li R, Xu L, Yao LZ (2017) DC fault detection and location in meshed multiterminal HVDC systems based on DC reactor voltage change rate. *IEEE Trans Power Deliv* 32(3):1516–1526
- [32] Zhang XP, Tai NL, Wang YH et al (2017) EMTR-based fault location for DC line in VSC-MTDC system using high-frequency currents. *IET Gen Transm Distrib* 11(10):2499–2507
- [33] Yang J, Fletcher JE, O'Reilly J (2012) Short-circuit and ground fault analyses and location in VSC-based DC network cables. *IEEE Trans Ind Electron* 59(10):3827–3837
- [34] Lin QZ, Luo GM, He JH (2017) Travelling-wave-based method for fault location in multi-terminal DC networks. *J Eng* 13:2314–2318
- [35] Leterme W, Azad SP, Hertem DV (2016) A local backup protection algorithm for HVDC grids. *IEEE Trans Power Deliv* 31(4):1767–1775
- [36] Xiang W, Hua Y, Wen JY et al (2014) Research on fast solid state DC breaker based on a natural current zero-crossing point. *J Mod Power Syst Clean Energy* 2(1):30–38
- [37] Ding X, Tang GF, Han MX et al (2018) Characteristic parameters extraction and application of the hybrid DC circuit breaker in MMC-HVDC. *Proc CSEE* 38(1):309–319
- [38] Ding X, Tang GF, Han MX et al (2018) Design and equivalence evaluation of type test for hybrid DC circuit breaker. *Power Syst Technol* 42(1):72–78

Xiangyu PEI received B.S. and M.S. degrees from Central South University, Hunan, China, in 2012 and Huazhong University of Science and Technology, Hubei, China, in 2015, respectively. Now, he is pursuing a Ph.D. degree in electrical engineering from the China Electric Power Research Institute (CEPRI), Beijing, China. His research interests include the protection and control of VSC-based HVDC grids.

Guangfu TANG received B.S. degree in electrical engineering from Xi'an Jiao Tong University, Xi'an, China, in 1990, and M.S. and Ph.D. degrees in electrical engineering from the Institute of Plasma Physics, the Chinese Academy of Sciences (ASIPP), Hefei, China, in 1993 and 1996, respectively. Now, he is an academician of the Chinese Academy of Engineering and vice president of the Global Energy Interconnection Research Institute (GEIRI), Beijing, China. His research interests include flexible AC transmission systems (FACTS), the converter valve of high voltage and ultra-high voltage in DC transmission systems, voltage-source converter-based high-voltage DC (VSC-HVDC) transmission systems, and DC grid.

Shengmei ZHANG received B.S. degree from Northeast Electric Power University, Jilin, China, in 2016. Now, she is pursuing an M.S. degree in electrical engineering from North China Electric Power University, Beijing, China. Her research interests include protection and control of VSC-based HVDC grids.

